Causes of Transient Oxygen Protection and Hydrogen-Induced Degradation in Api 5l X65 Steel

Hubert A. A. Alvarez*, Arnaldo Del Franzz Alvarez G., Pedro J. A. Alvarez G., Diego A. H. Alvarez G.

[A.A.A]. Group / Crom Engenharia – Natal, Rio Grande do Norte, Brazil

***Corresponding Author**

DOI: https://doi.org/10.51244/IJRSI.2025.12120148

Received: 01 January 2026; Accepted: 06 January 2026; Published: 19 January 2026

Keywords: Hydrogen embrittlement, Oxygen passivation, Density of states (DOS), Fe–H bond weakening, API 5L X65 steel

ABSTRACT

This article analyzes the electronic causes by which the oxygen–iron (O–Fe) interaction inhibits hydrogen (H_2) permeation in API 5L X65 steels, which are candidates for hydrogen transportation infrastructures. It is demonstrated that oxygen, due to its high electron affinity and the stability of its 2p orbitals, electronically dominates the iron surface.

Through a quantum-level analysis based on fundamental periodic properties, it is shown that O(2p)–Fe(3d) hybridization induces charge redistribution and a downward shift of the d-band center, weakening the Fe–H bond. This effect reduces hydrogen adsorption, dissociation, solubility, and permeation in the near-surface layers of the steel.

However, this inhibition is transient: the intrinsic properties of hydrogen—its small atomic size, high diffusivity, reducing character, and the action of high pressures—allow the progressive degradation of the oxidized layer, restoring permeation and promoting embrittlement mechanisms.

From a quantum perspective, hydrogen exploits the high electronic density of states near the Fermi level to stabilize Fe–H bonds and electronically displace oxygen. This interaction explains its high solubility in the metal and its ability to overcome the initial barrier imposed by oxygen. Understanding this behavior provides a conceptual basis for the rational design of hydrogen-resistant steels through alloying strategies, surface passivation, and control of operating conditions.

INTRODUCTION

Hydrogen permeation in steels intended for hydrogen infrastructure is governed by the initial processes of H_2 adsorption and dissociation on the metallic surface, which determine the amount of hydrogen entering the material and its susceptibility to embrittlement. Experimental studies and first-principles calculations have demonstrated that adsorbed species with high electron affinity, such as oxygen, compete for active sites on iron surfaces, increasing the activation barriers for H_2 dissociation and partially and transiently reducing hydrogen ingress into the metal [1–6].

In API 5L X65 steels, surface oxygen acts as a partial electronic inhibitor of hydrogen permeation by modifying the surface chemistry and the electronic structure of iron. The high electronegativity of oxygen and the stability of its 2p orbitals favor strong O(2p)–Fe(3d) hybridization, which induces a downward shift of the d-band and reduces the density of electronic states near the Fermi level, thereby weakening hydrogen adsorption, dissociation, and solubility on partially oxidized surfaces [7,8].

As a consequence, the formation of an oxide film initially acts as a protective barrier, limiting hydrogen entry into the metal. However, this protection is transient, since the small atomic size, high diffusivity, and reducing character of hydrogen enable the progressive degradation of the oxide layer and the reactivation of hydrogen permeation and embrittlement mechanisms.

In this context, the present work identifies the fundamental physicochemical causes governing both oxygen-induced inhibition and hydrogen solubility in API 5L X65 steel through an integrated analysis of periodic properties, orbital hybridization, and electronic density of states (DOS). These results provide atomistic–electronic foundations for the rational design of materials with improved resistance to hydrogen embrittlement.

Electronic Dominance of Oxygen on Metallic Surfaces [9, 27, 59]

The dominance of adsorbed oxygen on metallic surfaces originates from its high electronegativity, large effective nuclear charge (Z_{eff}), and strong stabilization of O(2p) orbitals, which promote intense charge transfer and robust O(2p)–Fe(3d) hybridization [9]. This interaction induces a downward shift of the iron d-band center (ε_d), reducing the density of electronic states near the Fermi level and, consequently, the surface reactivity toward hydrogen.

As a result of this electronic downshift, hydrogen permeation is inhibited through three complementary mechanisms:

- Decrease in active d states for H_2 dissociation;
- Reduction in available electronic states for atomic hydrogen transport; and
- Stabilization of a passivating surface layer with covalent Fe–O character [9, 27, 59].

At the electronic level, oxygen adsorption generates deep O–Fe bonding states and partial occupation of antibonding states, shifting ε_d toward more negative energies and weakening the Fe–H hybridization responsible for H–H bond activation. This behavior is consistent with DFT calculations showing that surface reactivity is governed by the adsorbate–metal hybridization energy rather than solely by the density of states at the Fermi level [9].

Additionally, the inhibitory effect of oxygen is electronically analogous to the low reactivity of noble metals such as Au, whose nobility is associated with a deep d-band center and reduced metal–hydrogen overlap [27]. Similarly, oxygen adsorption induces an electronically “noble” behavior in iron toward hydrogen, confined to the near-surface layers and transient in nature [9, 27].

Overall, the electronic dominance of oxygen reconfigures the electronic structure of iron, imposing unfavorable conditions for hydrogen adsorption, dissociation, and permeation, in full agreement with the Hammer–Nørskov model and the electronic principles governing metallic surface reactivity (TABLE 1).

METHODOLOGY

Electronic–Structural Framework for Hydrogen Permeation in API 5L X65 [1–9, 15–23]

This work adopts a physics-based analytical methodology grounded in quantum solid-state theory and surface science [1–3], with the objective of identifying the electronic mechanisms responsible for the transient inhibition of hydrogen permeation in API 5L X65 steel [4–6].

This approach goes beyond purely phenomenological models by establishing causal relationships of electronic origin between oxygen-induced surface chemistry and the processes of hydrogen adsorption, dissociation, diffusion, and embrittlement.

ISSN No. 2321-2705 | DOI: 10.51244/IJRSI |Volume XII Issue XII December 2025

We demonstrate that the transient inhibition of hydrogen permeation has an essentially electronic origin, governed by periodic descriptors—effective nuclear charge (Z_{eff}), electronegativity, and orbital energies [15–17]—as well as by descriptors of the surface Fe d-band, which control the competitive adsorption of H and O [18–23].

O(2p)–Fe(3d) hybridization redistributes the d states of surface iron, decreasing their overlap with H(1s) orbitals and weakening H_2 adsorption and dissociation governed by H(1s)–Fe(3d) interactions [7,9].

Accordingly, analysis of the electronic density of states (DOS), together with the Hammer–Nørskov d-band center model, demonstrates that the downward shift of the d-band center (ε_d) toward more negative energies acts as a unified and predictive electronic descriptor of oxygen-induced control over hydrogen adsorption, dissociation, and permeation [8,9].

Methodological Sequence [24–32]

The developed methodology follows a multiscale analytical sequence aimed at identifying the electronic origin of oxygen-induced inhibition of hydrogen permeation in API 5L X65 steels:

O–H electronic competition on the Fe surface

The initial competition between oxygen and hydrogen for active sites on the iron surface was analyzed using fundamental periodic descriptors and orbital energies, demonstrating the higher electron affinity of oxygen and the dominance of its 2p orbitals in O–Fe interactions [24,25].

Oxygen-induced surface electronic reconfiguration

Oxygen adsorption on the Fe surface induces strong O(2p)–Fe(3d) hybridization and significant charge redistribution, quantified through a downward shift of the d-band center. This effect reduces the electronic density of states near the Fermi level, modifying the surface reactivity of the steel [26,27].

Electronic–energetic correlation and effects on hydrogen

Shifts in the d-band center (ε_d) were correlated with DOS redistribution and with reductions in hydrogen adsorption and dissociation energies, leading to a regime of weakened or inhibited hydrogen adsorption in the near-surface layers of the material [28,29].

Extension into the bulk

The electronic redistribution induced by O–Fe surface interactions does not remain localized but propagates into the near-surface bulk, altering the energy landscape governing effective hydrogen solubility and diffusion. This electronic modification conditions hydrogen interactions with crystalline defects and microstructural traps, directly influencing transport and accumulation mechanisms in the steel [30–32].

Quantum-Mechanical Framework and Parameters

Quantitative analysis is supported by DFT calculations within the GGA approximation, widely used to describe electronic structure and adsorption energies on metallic surfaces [33].

The Hammer–Nørskov model constitutes the conceptual core linking the position of the d-band center to adsorption strength through adsorbate–metal hybridization [9,28]. Its theoretical basis lies in the Newns–Anderson formalism, which defines the d-band center (ε_d) as an operational and quantitative descriptor of surface reactivity [34–36].

For Fe surfaces, representative values are adopted:

ε_d (clean Fe): ≈ −0.92 eV [60]

ε_d (oxidized Fe): ≈ −2.5 eV [41–43]

This shift directly quantifies the oxygen-induced reduction in hydrogen reactivity. DFT calculations confirm a direct correlation between the d-band center (ε_d) and the hydrogen solution energy, demonstrating that a more negative ε_d effectively suppresses Fe–H interactions [41–43].

Hydrogen diffusion is modeled using Fick's law incorporating microstructural trapping effects [43]. Traps with a binding energy of approximately 28.4 kJ·mol^{-1} and a density of ≈ 6.84 × 10^{26} sites·m^{-3} are considered, representative of ferritic and high-strength API steels [43–45].

DFT calculations show strong hydrogen adsorption on clean Fe surfaces (E_{ads} ≈ −2.5 eV), whereas the presence of oxygen significantly reduces the adsorption energy (≈ −0.2 to −0.5 eV), consistent with the downward shift of ε_d [46]. Experimentally, O_2 concentrations between 100 and 12,000 ppm induce reductions in hydrogen permeation flux of 10–20%, confirming the electronic nature of the transient protective effect [45–47].

Theoretical Foundation – Hammer–Nørskov Model

The Hammer–Nørskov model, proposed in 1995 on the basis of DFT calculations, establishes a direct relationship between the catalytic activity of transition metals and the position of the d-band center (ε_d) relative to the Fermi level (E_F) [26]. This approach enables the rationalization and prediction of adsorption trends and surface reactivity using a simple electronic descriptor, without the need for full electronic structure calculations.

Electronic Origin of the Model

In transition metals, the overlap of d orbitals from neighboring atoms gives rise to a partially filled d band that dominates surface chemistry. The d-band center (ε_d), defined as the energy average of the d-projected density of states, effectively summarizes the occupation, availability, and hybridization capacity of these states [26].

When ε_d lies close to E_F, a high availability of partially occupied d states exists, capable of hybridizing with adsorbate orbitals, thereby favoring strong adsorption. In contrast, an ε_d shifted to more negative energies implies a largely filled d band, increases the occupation of antibonding states upon hybridization, and leads to weak adsorption [63]. This framework is consistent with classical solid-state physics results, which show that the electronic activity of d states depends critically on their proximity to E_F and on s–d coupling [63].

Mechanistic Interpretation: Newns–Anderson Formalism

From a mechanistic perspective, the metal–adsorbate interaction can be described using the Newns–Anderson formalism, in which adsorbate orbitals hybridize with metal d states, generating bonding and antibonding states [26]. The chemisorption energy is governed by the energetic separation and relative occupation of these states, with the occupation of antibonding states being the key factor that weakens adsorption.

The degree of hybridization and the resulting occupation depend on the energetic position of the d states relative to E_F. In this context, ε_d emerges as an effective descriptor that encapsulates both the hybridization strength and the occupation of states generated by the metal–adsorbate interaction [26,63].

Relationship Between Adsorption Energy and the d-Band Center

As a first approximation, the adsorption energy (ΔE_{ads}) correlates with the position of the d-band center according to the relationship:

$$\Delta E_{ads} \propto (E_F - \varepsilon_d)$$

When the d-band center (ε_d) lies close to the Fermi level (E_F), the occupation of antibonding metal–adsorbate states is reduced, which strengthens the metal–adsorbate bond and enhances adsorption. In contrast, a deeper εd\varepsilon_dεd increases the filling of antibonding states, thereby weakening the interaction and decreasing the adsorption strength [26]. This electronic framework underpins the formation of volcano-type activity plots

and provides the fundamental basis of the Sabatier principle, which is widely employed to rationalize and predict catalytic activity [26,63]

Validation of the Model

DFT calculations show that, with increasing atomic number and progressive filling of the d band, the d-band center ($\varepsilon_d - E_F$) systematically shifts toward more negative energies, reducing the availability of active d states [27]. Within the Hammer–Nørskov framework, this shift explains the transition from strong adsorption (Fe, Co), through an optimal regime of maximum activity (Ni, Ru, Rh, Pd, Pt), to weak adsorption in noble metals (Cu, Ag, Au) [27,28].

DFT studies on H_2 dissociation confirm that the low reactivity of Cu and Au originates from the high occupation of antibonding states and reduced metal–adsorbate orbital overlap, whereas metals with intermediate ε_d values exhibit optimal electronic conditions for hydrogen activation [27]. These evidences consolidate ε_d as a robust and universal descriptor of surface reactivity in transition metals (Table 2).

Periodic Trends

Table 2 and Figure 1 confirm that ε_d decreases systematically with atomic number across the 3d, 4d, and 5d series, with deviations associated with relativistic effects in heavy elements. Collectively, these results demonstrate that ε_d is an intrinsic electronic descriptor derived from the quantum structure of the d band, and that catalytic activity emerges directly from the electronic structure of the metal (Figure 1).

DISCUSSION

Therefore, oxygen adsorption on API 5L X65 steel initially inhibits interaction with hydrogen by inducing a downward shift of the Fe d-band center (ε_d) and reducing the electronic density of states near the Fermi level. However, this protective effect is transient: subsequent Fe–H interaction reorganizes the density of states (DOS), weakens surface Fe–O species, and reactivates the mechanisms of hydrogen adsorption, diffusion, and embrittlement. This behavior is consistently interpreted within the framework of the Hammer–Nørskov model and the Newns–Anderson formalism.

Electronic Mechanism of Oxygen

Oxygen adsorption profoundly modifies the surface electronic structure of iron, inhibiting H_2 activation. According to the Hammer–Nørskov d-band model, the presence of oxygen induces a downshift of ε_d, decreasing the availability of active d states for H(1s)–Fe(3d) hybridization [27]. This effect is electronically analogous to the low reactivity of noble metals such as Cu and Au, in which the high occupation of antibonding states and reduced orbital overlap limit hydrogen adsorption and dissociation [35].

From a mechanistic perspective, the Newns–Anderson formalism describes this inhibition as a consequence of reduced energetic separation between bonding and antibonding metal–adsorbate states and a more unfavorable antibonding occupation, which weakens hydrogen chemisorption [36]. DFT calculations confirm that electronegative adsorbates induce downshifts of ε_d even in the absence of geometric effects, acting as long-range electronic modifiers of Fe surface reactivity.

Metal–Oxygen Interaction and d-Band Downshift

Hybridization between O(2p) and Fe(3d) orbitals induces significant electronic redistribution at the iron surface, with the formation of deep bonding states and partially occupied antibonding states. In clean iron, the d-band center is located at $\varepsilon_d \approx -0.92$ eV; upon oxygen adsorption, ε_d shifts to approximately −2.5 eV, reducing the density of states near the Fermi level and weakening hydrogen adsorption [8,61,28].

This downshift originates from the strong energetic misalignment between O(2p) and Fe(3d) orbitals, which favors charge transfer toward oxygen and stabilizes O–Fe bonds [37]. Conceptually, this shift acts as an

"electronic switch" of surface reactivity: by moving d states away from E_F, hybridization with H(1s) orbitals is limited and preferential stabilization of oxygen over hydrogen is promoted.

Electronic and energetic descriptors quantify this effect by correlating ε_d and the DOS with adsorption strength and reactivity, enabling prediction of hydrogen behavior trends in 3d metals and alloys [38]. DFT studies show that reactivity does not depend solely on the density of states at E_F, but on the hybridization energy between bonding/antibonding adsorbate states and the metal d band, confirming the validity of ε_d as an electronic descriptor [39]. Figure 2 schematically illustrates this mechanism and its impact on the electronic density of states, consolidating the role of oxygen as a long-range electronic modifier on iron surfaces (Figure 2).

Dissociative Adsorption of O_2 [28, 48]

Molecular oxygen adsorbs dissociatively on Fe surfaces in API X65 steels, preferentially occupying hollow and bridge sites. Its high electronegativity and small atomic radius favor the formation of strongly polar Fe–O bonds, with charge transfer on the order of 0.5–1 e per oxygen atom.

Thermodynamically, oxygen adsorption is highly favorable (−5 to −6 eV), far exceeding that of hydrogen (≈ −0.5 eV), ensuring preferential occupation of active sites even under H_2/O_2 competition [37]. From a kinetic standpoint, O_2 dissociation exhibits low activation barriers (≈ 0.2–0.5 eV) due to efficient hybridization between O_2 π orbitals and Fe d states, leading to rapid formation of ordered monolayers such as the p(2×2)-O phase on Fe surfaces (Figure 3) [28].

Conceptually, surface reactivity depends not only on the density of states at E_F, but on the hybridization energy between bonding and antibonding adsorbate states and the metal d band, as supported by DFT calculations and activation barrier estimates [48]. This relationship explains the rapid dissociation of O_2 and the stability of oxygen adsorption against hydrogen, reinforcing the predictive capability of electronic and energetic descriptors for surface behavior [28,48] (Figure 3).

Electronic Modification and Density of States (DOS) [9, 49, 62]

Oxygen adsorption on Fe induces intense O(2p)–Fe(3d) hybridization, redistributing surface electronic density and transferring charge from the metal to the adsorbate. This coupling generates deep bonding states and antibonding states near the Fermi level, weakening subsequent interactions such as Fe–H bonding. The greater strength of the O–Fe bond (2–3 eV) relative to H–Fe (~0.5 eV) dominates the electronic response of the first surface layers, inducing a downshift of the d-band center (ε_d), reducing hydrogen adsorption energy (from ~−0.5 to ~−0.2 eV), and increasing the H_2 dissociation barrier above 1 eV [9].

This phenomenon can be explained by the d-band model and the relationship between metal d states and adsorbate orbitals: greater filling of antibonding states and the position of ε_d relative to E_F determine bond strength and surface reactivity [9]. Recent DFT studies on O_2 activation on metallic surfaces confirm that oxygen reactivity and oxide formation tendency correlate with the position and density of d states; surfaces with a more filled and lower-energy d band exhibit inert behavior, whereas open or defective sites show high reactivity [49].

This framework reinforces that chemisorption of electronegative adsorbates induces electronic redistribution, with the formation of deep bonding states (~2–3 eV below E_F) and increased occupation of antibonding states. The neighboring d-band downshift (1–2 eV) reduces hydrogen adsorption energy and raises H_2 dissociation barriers, reflecting weaker metal–adsorbate hybridization and a second-order electronic response of the surface layers, in agreement with DOS redistribution and electronic blocking of active sites [62].

As a result, hydrogen adsorption, solubility, and permeation are significantly reduced, establishing an electronic blocking of active sites that limits hydrogen mobility and mitigates hydrogen embrittlement in API X65 steels.

Figure 4 illustrates how an adsorbate (such as oxygen) interacts with the metal s and d orbitals, forming bonding and antibonding states. The position of these states relative to the Fermi level defines adsorption strength and governs changes in surface reactivity (Figure 4).

H_2 Activity in the Presence of Oxygen Inhibition in API X65 Steel [50–52]

Molecular hydrogen (H_2) progressively overcomes the initial oxygen-induced inhibition in API X65 steels through a combination of electronic, thermodynamic, and kinetic effects that degrade the surface O/Fe–O layer. Although adsorbed oxygen induces a downshift of the d-band center and increases the barriers for hydrogen adsorption and diffusion, this layer is thin, discontinuous, and susceptible to chemical reduction by H_2 [50]. The competitive conversion of FeO species into OH* and H_2O weakens oxide stability, allowing hydrogen to penetrate into the metallic matrix [51].

The small atomic radius of hydrogen, its high diffusivity in α-ferrite, and high operating pressures favor interstitial transport. Experimental studies show that hydrogen solubility and diffusion are governed by activation toward octahedral sites and by dislocation-assisted diffusion (pipe diffusion), further facilitated by hydrogen-induced plasticity mechanisms [50,51]. Once the surface barrier is compromised, interstitial diffusion dominates and activates embrittlement mechanisms such as HEDE and HELP, particularly in microstructures subjected to deformation or thermal treatments [52].

From an electronic standpoint, the overcoming of oxidizing inhibition is explained by the reorganization of the Fe density of states during hydrogen adsorption. Fe–H hybridization generates bonding states near the Fermi level, restoring surface reactivity and revealing the transient nature of oxygen-induced protection. In this context, the effectiveness of oxygen depends critically on the electronic competition between H and O for d states near E_F [50–52].

Fe–H vs. Fe–O Competition: Electronic Basis for Hydrogen Penetration [50, 54–58]

Hydrogen inhibition by oxygen or oxides on iron is intrinsically transient and arises from electronic competition around the Fermi level. Metallic Fe exhibits a high density of d states near E_F, which favors hybridization with H(1s) orbitals and the formation of electronically stabilized Fe–H bonds [50,55,56]. In contrast to oxygen, whose 2p states lie at deep energies and are largely decoupled from E_F, hydrogen interacts efficiently with Fe 3d, 4s, and 4p states, lowering kinetic barriers and promoting high interstitial mobility [55,56].

This Fe–H hybridization stabilizes bonding states near E_F and reduces the total energy of the system more effectively than Fe–O bond formation, thermodynamically favoring hydrogen dissolution, particularly under high H_2 partial pressures [50,54]. DFT calculations and experimental studies show that hydrogen preferentially adsorbs at high-coordination sites on Fe with low diffusion barriers, while H_2 can reduce partially oxidized surfaces and displace adsorbed oxygen [56,57].

Overall, the high availability of electronic states near E_F, Fe–H hybridization, interstitial diffusion, and Fe–O electronic competition explain the breakdown of the oxidized barrier and the transient nature of the initial inhibition. These effects facilitate hydrogen penetration, DOS reorganization, and activation of HEDE/HELP embrittlement mechanisms, as conceptually summarized in Table 3 and Figure 5 [50,54–58].

CONCLUSIONS

Based on the above analysis, the transient inhibition of hydrogen permeation induced by oxygen in API X65 steel can be coherently explained by quantum-mechanical mechanisms, particularly O(2p)–Fe(3d) hybridization and the associated electronic redistribution evidenced in the band structure, Fermi level, and density of states (DOS). The formation of Fe–O bonds shifts the d-band center toward lower energies and reduces the DOS near the Fermi level, generating an initial electronic barrier that limits hydrogen adsorption and activation.

Nevertheless, this protection is partial and non-permanent, since the small atomic size, high diffusivity, and reducing character of hydrogen enable it to progressively overcome this barrier and restore permeation within the metallic lattice.

From a materials design perspective, and based on the results of this work, a rational strategy is established to improve hydrogen resistance in X65 steels. This strategy includes controlled alloying (Cr, Mo, and Ni), the use

of protective coatings, control of operating conditions, and DFT-based electronic modeling, all aimed at reducing surface reactivity toward hydrogen and increasing material stability in green hydrogen applications.

In summary, the fundamental mechanisms and derived strategies, summarized in **Table 4**, provide a quantitative and conceptual basis for the optimization of API X65 steels intended for hydrogen-based energy infrastructures.

BIBLIOGRAPHY

1. Staykov, A., Yamabe, J., & Somerday, B. P. (2014).,Effect of hydrogen gas impurities on the hydrogen dissociation on iron surface.,Int. J. Quantum Chemistry, 114(10), 626–635., https://doi.org/10.1002/qua.24633
2. Staykov, A., Komoda, R., Kubota, M., & Watanabe, S. (2019).
3. Coadsorption of CO and H_2 on an iron surface and its implication on hydrogen embrittlement of iron.,The Journal of Physical Chemistry C, 123(50), 30265–30273.https://doi.org/10.1021/acs.jpcc.9b06927
4. Zhang, N., Wada, K., Komoda, R., Staykov, A., & Kubota, M. (2025).
5. Kinetic modeling of ammonia and hydrogen dissociative co-adsorption on iron surface and its effect on hydrogen embrittlement., Physical Chemistry Chemical Physics, 27, 24589–24600. https://doi.org/10.1039/D5CP02423D
6. Röthig, M., Hoschke, J., Chowdhury, M. F. W., Tapia-Bastidas, C. V., Venezuela, J., Gray, E., & Atrens, A. (2025).,Gaseous hydrogen permeation in X65 D pipeline steel and a preliminary evaluation of the influence of oxygen.,Int. J. Hydrogen Energy, 158, 150459., https://doi.org/10.1016/j.ijhydene.2025.150459
7. Sun, Y., & Cheng, F. (2024).,Dissociative adsorption of hydrogen molecules at Al_2O_3 inclusions in steels and its implications for gaseous hydrogen embrittlement of pipelines., Corrosion and Materials Degradation, 5(2), 200–223., https://doi.org/10.3390/cmd5020008
8. Youhan, U. K., & Koehler, S. P. K. (2021)., Energetics of hydrogen adsorption and diffusion for the main surface planes and all magnetic structures of γ-iron using DFT.,RSC Advances, 11, 28892–28897., https://doi.org/10.1039/D1RA04999B
9. Yifan Ye, James Thorne, Cheng Hao Wu., Yi-Sheng Liu., Chun Du., Ji-Wook Jang., Erik Liu., Dunwei Wang., Jinghua Guo., Strong O 2p-Fe 3d Hybridization Observed in Solution-Grown Hematite Films by Soft X-ray Spectroscopies.,J. Phys. Chem. B 2018, 122, 2, 927–932., https://doi.org/10.1021/acs.jpcb.7b06989
10. Mogamat A. Peck; David Santos-Carballal; Nora H. de Leeuw; Michael Claeys., Density Functional Theory Study of the Adsorption of Oxygen and Hydrogen on 3d Transition Metal Surfaces with Varying Magnetic Ordering., S.Afr.j.chem. (Online) vol.74. Durban 2021., https://doi.org/10.17159/0379-4350/2021/v74a11
11. B. Hammer, J. K. Nørskov, Electronic factors determining the reactivity of metal surfaces, **Surface Science**, 343, 211–220 (1995)., 10.1016/0039-6028(96)80007-0
12. E. Clementi, D. L. Raimondi, and W. P. Reinhardt., Atomic Screening Constants from SCF Functions. II. Atoms with 37 to 86 Electrons: J. Chem. Phys. 47, 1300 (1967); doi: 10.1063/1.1712084., i) http://dx.doi.org/10.1063/1.1712084,
13. Pauling, L. The Nature of the Chemical Bond. Cornell University Press.,Tablas complementarias: WebElements (O y Ni).,https://www.webelements.com
14. NIST Atomic Spectra Database – Ionization Energies., https://physics.nist.gov/PhysRefData/ASD/ionEnergy.html
15. Slater, J. C.“Atomic Radii in Crystals.”.,J. Chem. Phys. 1964, 41, 3199.https://doi.org/10.1063/1.1725697
16. Hüfner, S.,“Photoelectron Spectroscopy: Principles and Applications.” Springer, 3rd edition, 2003. ISBN 3-540-60875-3 2nd Edition Springer-Verlag Berlin Heidelberg New York
17. Nazmul Islam, Dulal C. Ghosh, The Electronegativity and the Global Hardness Are Periodic Properties of Atoms, **Journal of Quantum Information Science**, 2011, 1, 135–141. https://doi.org/10.4236/jqis.2011.13019

18. Sangjoon Lee, Clio Chen, Griheydi Garcia, Anton Oliynyk, Machine learning descriptors in materials chemistry used in multiple experimentally validated studies: Oliynyk elemental property dataset, **Data in Brief**, Volume 53, April 2024, 110178. https://doi.org/10.1016/j.dib.2024.110178
19. Lindsey N. Anderson, M. Belén Oviedo, Bryan M. Wong, Accurate Electron Affinities and Orbital Energies of Anions from a Non-Empirically Tuned Range-Separated Density Functional Theory Approach, **Journal of Chemical Theory and Computation**, 13, 1656 (2017). https://doi.org/10.1021/acs.jctc.6b01249
20. J. Hu, Adel Al-Salihy, B.Zhang, S.Li, P. Xu., Mastering the D-Band Center of Iron-Series Metal-Based Electrocatalysts for Enhanced Electrocatalytic Water Splitting., Int J Mol Sci. 2022 Dec 6;23(23):15405. doi:10.3390/ijms232315405https://doi.org/10.3390/ijms232315405
21. Bhattacharjee, S.; Waghmare, U. V.; Lee, S.-C.,An improved d-band model of the catalytic activity of magnetic transition metal surfaces.,Scientific Reports, 6, 35916 (2016)., https://doi.org/10.1038/srep35916
22. Ruban, A.; Hammer, B.; Stoltze, P.; Skriver, H. L.; Nørskov, J. K.,Surface electronic structure and reactivity of transition and noble metals.,Journal of Molecular Catalysis A: Chemical, 115 (3), 421–429 (1997).,https://doi.org/10.1016/S1381-1169(96)00348-2
23. Ossowski, T.; Kiejna, A.,Oxygen adsorption on Fe(110) surface revisited, Surface Science, 637–638, 35–41 (2015).,https://doi.org/10.1016/j.susc.2015.03.001
24. Wang, T.; Wang, S.; Luo, Q.; Li, Y.-W.; Wang, J.; Beller, M.; Jia, H.,Hydrogen adsorption structures and energetics on iron surfaces at high coverage.,The Journal of Physical Chemistry C, 118, 2014. DOI: 10.1021/jp410635z, https://doi.org/10.1021/jp410635z
25. Xin, H.; Vojvodic, A.; Voss, J.; Nørskov, J. K.; Abild-Pedersen, F., Effects of d-band shape on the surface reactivity of transition-metal alloys.Physical Review B, 89 (11), 115114 (2014).,https://doi.org/10.1103/PhysRevB.89.115114
26. Peck, M. A.; Santos-Carballal, D.; de Leeuw, N. H.; Claeys, M.,Density Functional Theory Study of the Adsorption of Oxygen and Hydrogen on 3d Transition Metal Surfaces with Varying Magnetic Ordering., **South African Journal of Chemistry 2021**, 74, Article a11., https://doi.org/10.17159/0379-4350/2021/v74a11
27. Zhang, S.; Li, K.; Ma, Y.; Bu, Y.; Liang, Z.; Yang, Z.; Zhang, J., The Adsorption Mechanism of Hydrogen on FeO Crystal Surfaces: A Density Functional Theory Study., **Nanomaterials 2023**, 13 (14), 2051., https://doi.org/10.3390/nano13142051
28. D. M. Newns, Self-consistent model of hydrogen chemisorption on transition metals, Phys. Rev. 178, 1123 (1969). https://doi.org/10.1103/PhysRev.178.1123
29. Greeley, J.; Nørskov, J. K. Large-scale, density functional theory-based screening of alloys for hydrogen evolution. Surface Science 2007, 601 (6), 1590–1598., DOI: https://doi.org/10.1016/j.susc.2007.01.037
30. B. Hammer, J. K. Nørskov, Theoretical surface science and catalysis — calculations and concepts, Adv. Catal. 45, 71 (2000). https://doi.org/10.1016/S0360-0564(02)45013-4
31. Kitchin et al. (J. Chem. Phys. 2004) / Takigawa 2016. backend.orbit.dtu.dk+1
32. Islam, A.; Li, Q.; Storimans, E.; Ton, K.; Alam, T.; Farhat, Z. N., Effect of Microstructure on Hydrogen Permeation and Trapping in Natural Gas Pipeline Steels., **npj Mater. Degrad. 2025**, 9, 70., https://doi.org/10.1038/s41529-025-00615-5
33. Li, Y.; Wei, H.; Zheng, S.; Kong, J.; Wen, L.; Yuan, Q.; Liu, Y.; Shen, Y.; Zhang, Y.; Wu, H.; Zhou, L.; Shen, G.; Domblesky, J. P.; Hussain, G.; Ostrikov, K. (Ken)., Hydrogen Adsorption and Diffusion on the Surface of Alloyed Steel: First-Principles Studies., **Int. J. Hydrogen Energy 2024**, 54, 1478–1486., https://doi.org/10.1016/j.ijhydene.2023.12.046
34. Devi, A. A. S.; Javaheri, V.; Pallaspuro, S.; Komi, J., First-Principles Insights into Hydrogen Interaction with Alloyed Surfaces., **Phys. Chem. Chem. Phys. 2024**, 26, 26222–26237., https://doi.org/10.1039/D4CP02233E
35. Takigawa 2016 / revisiones. eprints.lib.hokudai.ac.jp+1
36. Sebastian Schnur and Axel Gro . Strain and coordination e ects in the adsorption properties of early transition metals Institut fur Theoretische Chemie, Universitat Ulm, D-89069 Ulm, German., Early_dband_metals_dist.pdf
37. Hammer, J. K. Nørskov, Why gold is the noblest of all the metals, **Nature** 376, 238–240 (1995).,https://doi.org/10.1038/376238a0

38. D. M. Newns, Self-consistent model of hydrogen chemisorption on transition metals, **Phys. Rev.** 178, 1123–1135 (1969).,https://doi.org/10.1103/PhysRev.178.1123
39. J. R. Kitchin et al., J. Chem. Phys., 2004., Modification of the surface electronic and chemical properties of Pt(111) by subsurface transition metals., J. Chem. Phys. 120, 10240–10246 (2004)., Kit.pdf
40. Nørskov et al., J. Catal., 2008 (aplicaciones catalíticas); S. Hüfner, Photoelectron Spectroscopy (análisis p-d)., https://scispace.com/pdf/using-photoelectron-spectroscopy-and-quantum-mechanics-to-1hirrypw08.pdf., https://doi.org/10.1016/j.isci.2025.113080
41. B. Hammer and J. K. Nørskov, Electronic factors determining the reactivity of metal surfaces. Surface Science 343, 211–220 (1995).,https://doi.org/10.1016/0039-6028(96)80007-0
42. Jing Hu, A. Al-Salihy, B. Zhang, S. Li, P. Xu., Mastering the D-Band Center of Iron-Series Metal-Based Electrocatalysts for Enhanced Electrocatalytic Water Splitting., Int J Mol Sci. 2022 Dec 6;23(23):15405. , https://doi.org/10.3390/ijms232315405
43. Q. Zhu, W.Huang, C.Huang, L. Gao,Y. Su, L.Qiao., The d band center as an indicator for the hydrogen solution and diffusion behaviors in transition metals., International Journal of Hydrogen Energy. Volume 47, Issue 90,(2022), Pages 38445-38454, https://doi.org/10.1016/j.ijhydene.2022.09.021
44. F. Xie, C. Yuan, H.Tan, A.Z. Moshfegh, B. Zhu, J. Yu., d-Band Center Regulated O_2 Adsorption on Transition Metal Single Atoms Loaded COF: A DFT Study., Acta Physico-Chimica Sinica Volume 40, Issue 11,(2024), 2407013., https://doi.org/10.3866/PKU.WHXB202407013
45. Drexler, M. Galler, H. Elsayed, R. Vallant, C. Sommitsch., Critical verification of the effective diffusion concept, International Journal of Hydrogen Energy Volume 48, Issue 20, (2023), Pages 7499-7514., https://doi.org/10.1016/j.ijhydene.2022.11.105
A. Drexler, S. Pastore, J. Domitner., Modeling bulk diffusion of hydrogen in X70 pipeline steel., Scientific Reports volume 15, 6363 (2025)., https://doi.org/10.1038/s41598-025-90130-z
46. .D. Mallick, N. Mary, V. S. Raja, B. Normand., Study of Diffusible Behavior of Hydrogen in First Generation Advanced High Strength Steels., Metals 2021, 11, 782. https://doi.org/10.3390/met11050782
47. N. Venkata S. Korlapati,F. Khan, S. Vaddiraju, T. Cagin., Hydrogen diffusion dynamics on Fe(100) surface: A mechanism of hydrogen-induced failure., International Journal of Hydrogen Energy Volume 65, (2024), Pages 177-185
48. T. Tanabe, Y. Yamanishi, S. Imoto., Hydrogen Transport through Highly Purified Iron., Transactions of the Japan Institute of Metals 25(1):1-10., DOI:10.2320/matertrans1960.25.1
49. Ulrike Diebold., Surface Science Reports 48 (2003) 53–229., https://nathan.instras.com/documentDB/paper-38.pdf
50. M. M. Montemore., M. A. van Spronsen., R. J. Madix., C. M. Friend., O_2 Activation by Metal Surfaces: Implications for Bonding and Reactivity on Heterogeneous Catalysts., Chem. Rev. 2018, 118, 5, 2816–2862., https://doi.org/10.1021/acs.chemrev.7b00217
51. K. Kiuchi, R. B. McLellan, The solubility and diffusivity of hydrogen in well-annealed iron, Acta Metallurgica, 31, 961–984 (1983)..,https://doi.org/10.1016/0001-6160(83)90192-X
52. H. K. Birnbaum, P. Sofronis, Hydrogen-enhanced localized plasticity — a mechanism for hydrogen-related fracture, Materials Science and Engineering A, 176, 191–202 (1994)., https://doi.org/10.1016/0921-5093(94)90975-X
53. Sieverts (1929); Röthig et al. (2025). Absorption of gases by metals.,https://link.springer.com/article/10.1007/s11661-010-0394-0
54. Gangloff, R. P..,Hydrogen Embrittlement., ASM Handbook, Volume 13: CorrosionDOI: 10.31399/asm.hb.v13.9781627081899.,.,https://dl.asminternational.org/handbooks/book/12/asm-handbook-volume-13a-corrosion-fundamentals
55. Marcolongo, S. Zulueta, T. A. Pham., The role of density functional theory in decoding the complexities of hydrogen embrittlement in steels. Phys. Chem. Chem. Phys. 2024. DOI: 10.1039/D4CP02233E., https://pubs.rsc.org/en/content/articlelanding/2024/cp/d4cp02233e
56. Y. Jiang, T. J. Rauguth, J. G. Che., Surface Structure and Energetics of Hydrogen Adsorption on the Fe(110) Surface., DOI: 10.1021/jp051907s., PubMed: 16852778., https://pubs.acs.org/doi/10.1021/jp051907s
57. M. A. Niyaz, A. B. A. R. Hafiz, K. M. M. D. H. Islam., Advances., DOI: 10.1039/D1RA04999B.,https://pubs.rsc.org/en/content/articlelanding/2021/ra/d1ra04999b

58. L. Wang, X. Zhang, H. Liu., The Adsorption Mechanism of Hydrogen on FeO Crystal Surfaces: A Density Functional Theory Study. Nanomaterials 2023. DOI: 10.3390/nano13142051.,https://www.mdpi.com/2079-4991/13/14/2051
59. Y. Li, L. Wang, H. Wang, X. Shu.,First-principles study of interactions of oxygen–carbon–vacancy in bcc Fe., Chinese Physics B., 2019, 28(10), 106102.,https://doi.org/10.1088/1674-1056/ab3a8f
60. B., Xing, J. Wu, J. Cheng, L. Zhang, M.Wu., Hydrogen diffusion in α-Fe_2O_3: Implication for an effective hydrogen diffusion barrier., Int.Journal of Hydrogen Energy., V(45), Issue 56, November 2020, Pages 32648-32653., **https://doi.org/10.1016/j.ijhydene.2020.08.263**
61. Nørskov dataset / Takigawa 2016. eprints.lib.hokudai.ac.jp
62. Vojvodic, A.; Nørskov, J. K.; Abild-Pedersen, F. Electronic structure effects in transition metal surface chemistry. Topics in Catalysis 2014, 57 (1-4), 25–32.DOI: https://doi.org/10.1007/s11244-013-0159-2
63. S. Saini., J. H. Stenlid., F. A-Pedersen., Electronic structure factors and the importance of adsorbate effects in chemisorption on surface alloys., npj Computational Materials., **v(8)**, Article number:163 (2022)., https://doi.org/10.1038/s41524-022-00846-z
64. P. W. Anderson, Localized magnetic states in metals, Phys. Rev. 124, 41 (1961).https://doi.org/10.1103/PhysRev.124.41

Tablas (1-3)

Table 1. Values of Critical Periodic Properties (O vs. Fe) [10–14]

Property	**Oxygen (O)**	**Transition Metal (e.g., Iron, Fe)**	**Difference / Interpretation**
Effective Nuclear Charge (Z_eff)	2p ≈ 4.45 (very high)	4s ≈ 1.2–1.7 (estimated); 3d ≈ 6–7 (strongly shielded)	Oxygen exhibits a much higher Z_eff on its valence electrons → more contracted and stable orbitals. In Fe, 3d electrons are strongly shielded → more diffuse and more reactive. [10]
Electronegativity (Pauling)	3.44	1.83 (Fe)	$\Delta\chi \approx 1.6–1.7$ → strongly polar $O\delta^-$—$Fe\delta^+$ bond, favoring electron transfer toward oxygen. [11]
First Ionization Energy (IE_1)	1313.9 kJ·mol^{-1}	762.5 kJ·mol^{-1} (Fe)	Oxygen has a much higher IE → more stable valence orbitals, stronger nucleus–electron attraction. Fe ionizes more easily → acts as an electron donor. [12]
Atomic / Covalent Radius	≈ 66 pm (very small)	≈ 126 pm (Fe)	Oxygen is compact → high electronic density. Fe is larger and more diffuse → facilitates oxygen penetration, oxide formation, and surface reconstruction. [13]
Valence orbital energy level	2p orbital ≈ −14 to −15 eV (deep, highly stable potential well); H(1s) = −13.6 eV	3d/4s orbitals ≈ −6 to −8 eV (less stable)	$\Delta E \approx 7–9$ eV → oxygen strongly withdraws electronic density from Fe, explaining the d-band downshift, the formation of deep bonding states, and the spontaneous oxidation of the iron surface. [14]

ISSN No. 2321-2705 | DOI: 10.51244/IJRSI |Volume XII Issue XII December 2025

Table 2. Relationship between Z–εd–(d+s) and catalytic activity (Hammer–Nørskov model) for 3d, 4d, and 5d elements [60, 29, 33, 34]

Element	Atomic Number (Z)	εd − EF (eV) (DFT, diagonal)	Valence electrons (d + s)	Hammer–Nørskov interpretation (adsorption / catalysis)
Fe	26	−0.92	$3d^6 4s^2 \rightarrow 8$	d-band very close to EF → high DOS near EF. Strong donation/back-donation to adsorbates → strong bonds, low activation barriers (highly active for O_2 dissociation, H_2 activation, redox reactions).
Co	27	−1.17	$3d^7 4s^2 \rightarrow 9$	εd slightly deeper than Fe → high activity but somewhat lower; good adsorption and catalytic capability, similar behavior but less donating than Fe.
Ni	28	−1.29	$3d^8 4s^2 \rightarrow 10$	εd deeper than Co → reduced relative reactivity; still active for bonding with H, O, and CO; typically a good catalyst for partial hydrogenation.
Cu	29	−2.67	$3d^{10} 4s^1 \rightarrow 11$	d-band far from EF (very deep) → low surface activity / more noble behavior; weak adsorption compared with Fe–Ni.
Ru	44	−1.41	$4d^7 5s^1 \rightarrow 8$	εd relatively high (close to Ni/Co) → good balance between bond strength and stability; known for strong activity in hydrogen-related reactions and synthesis.
Rh	45	−1.73	$4d^8 5s^1 \rightarrow 9$	εd deeper than Ru → moderate-to-high activity; strong selective coupling with certain adsorbates (effective for hydrogenation).
Pd	46	−1.83	$4d^{10} 5s^0 \rightarrow 10$	Relatively deep d-band → less donating than Fe, but unique properties (subsurface H absorption, hydride-forming capability).
Ag	47	−4.30	$4d^{10} 5s^1 \rightarrow 11$	Very deep εd → noble metal; weak adsorption and low molecular activation capacity compared with Fe–Ru.
Ir	77	−2.11	$5d^7 6s^2 \rightarrow 9$	Moderately deep εd; combines stability with good catalytic performance in high-potential reactions (oxidation, selective hydrogenation).
Pt	78	−2.25	$5d^9 6s^1 \rightarrow 10$	Deep–moderate εd → highly active in practice (balance between adsorption and product release), but less donating than Fe.
Au	79	−3.56	$5d^{10} 6s^1 \rightarrow 11$	Deep εd → noble behavior; weak adsorption on flat surfaces; however, Au nanoparticles show activity due to size and coordination effects.

ISSN No. 2321-2705 | DOI: 10.51244/IJRSI |Volume XII Issue XII December 2025

Table 3. Graphical–conceptual summary of the process (clean Fe vs. Fe–H according to the DOS) [38, 58, 60-62]

Energy Region (eV)	**Band Name**	**Clean Fe (Blue)**	**Fe with adsorbed H (Red)**	**Physical Meaning**
Negative (< 0)	Valence Band	High DOS associated with Fe valence electrons (d and s orbitals).	New peaks appear corresponding to Fe–H bonding states; the DOS is redistributed.	Formation of the Fe–H chemical bond: electrons localize in bonding orbitals.
Zero (0)	Fermi Level (E_0)	Defines the boundary between occupied and unoccupied states; exhibits a high DOS peak.	DOS at E_0 decreases as electrons relax into bonding states.	Reduced surface metallic reactivity (fewer electrons available at E_0).
Positive (> 0)	Conduction Band	Unoccupied states available for electronic excitation.	DOS near E_0 remains reduced and stays lower than in clean Fe at higher energies.	Evidence of charge transfer and stabilization: electrons migrate to lower-energy states.

Table 4. Established quantum theories identifying the root cause of the problem

Established Quantum Theory	**Role in the Analysis**	**Root-Cause Explanation**
1. Orbital Theory / Hybridization	Explains the initial surface chemical interaction.	O(2p)–Fe(3d) hybridization redistributes the electronic density at the iron surface, creating a new electronic barrier.
2. d-Band Theory	Explains changes in surface reactivity.	The d-band downshift weakens Fe–H back-donation, reducing the adsorption and dissociation energies of H_2.
3. Periodic Properties (Z_eff, Electronegativity)	Explains the electronic dominance of oxygen.	The higher effective nuclear charge (Z_eff) and electronegativity of O allow it to dominate the interaction and withdraw electronic density from Fe.
4. Surface Adsorption Theory	Links electronic structure to macroscopic properties.	Quantitatively correlates the d-band position with adsorption energy, predicting weakening of the Fe–H_2 interaction.
5. Statistical Quantum Mechanics and Diffusion	Explains the transient nature of inhibition.	The minimal atomic radius and high diffusivity of H, governed by quantum effects, allow it to overcome the oxidized barrier over time under pressure.

Figuras (1 – 5)

ISSN No. 2321-2705 | DOI: 10.51244/IJRSI |Volume XII Issue XII December 2025

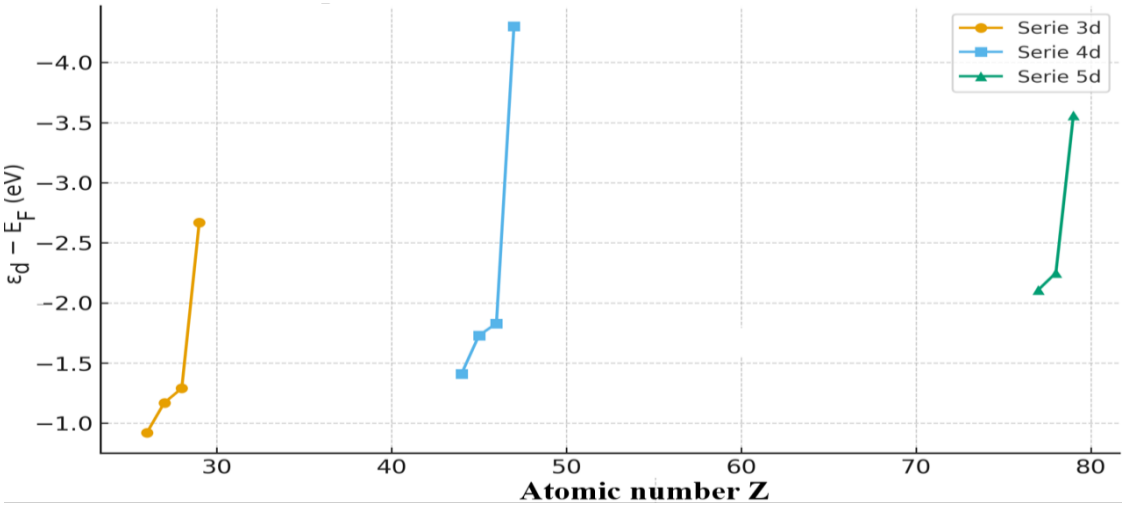

Figure 1. d-band center (ε_d − E_F) as a function of the atomic number Z for 3d, 4d, and 5d transition metals [19].

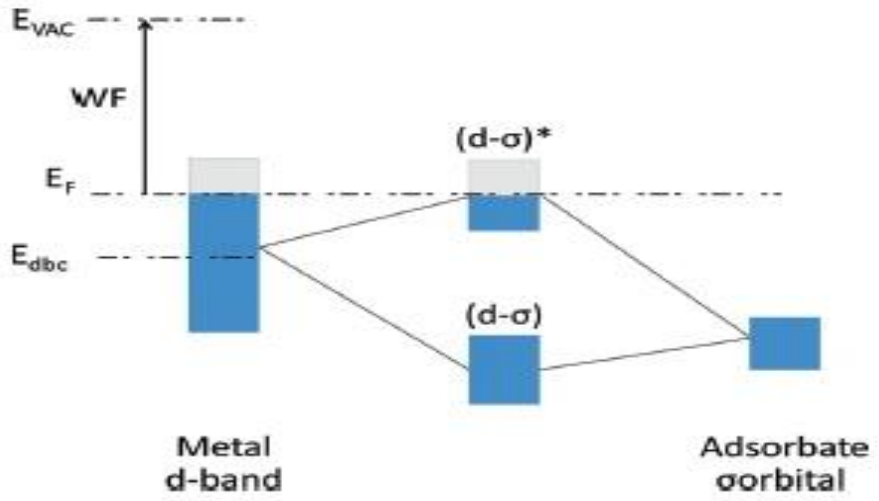

Figure 2. Schematic representation of the coupling between the metal d-band and the adsorbate orbital, illustrating the formation of bonding (d–σ) and antibonding (d–σ)* states [8].

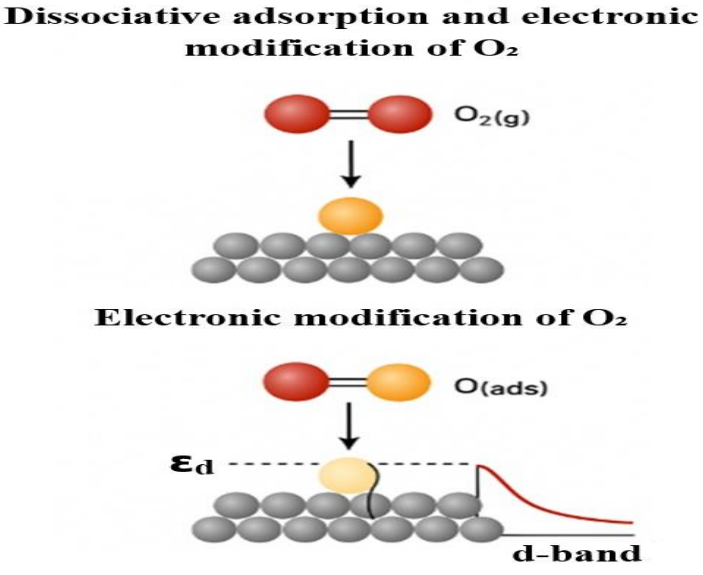

Figure 3. Dissociative adsorption and electronic modification of O_2 on the metal surface

ISSN No. 2321-2705 | DOI: 10.51244/IJRSI |Volume XII Issue XII December 2025

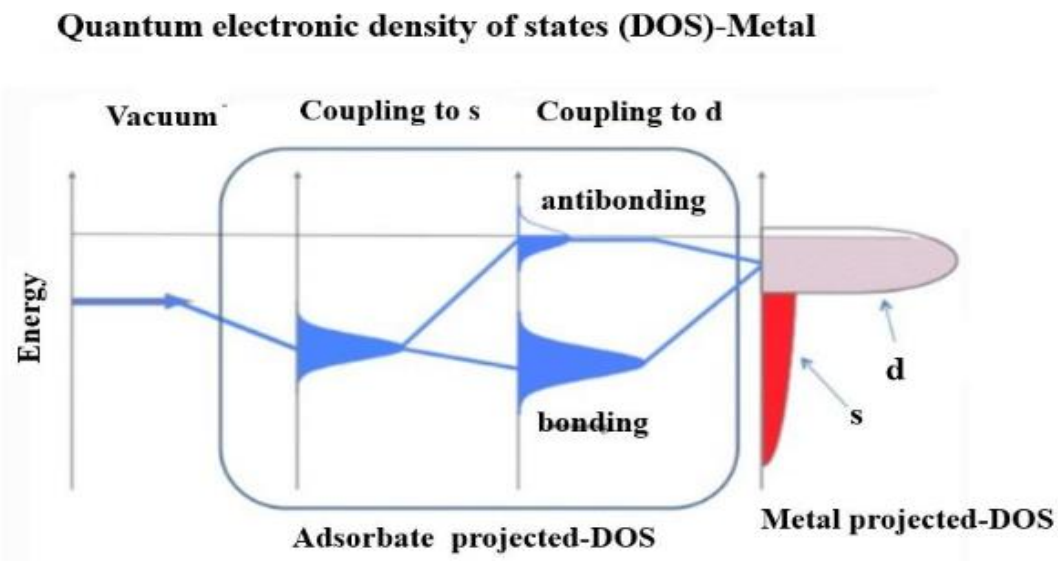

Figure 4.-Quantum electronic density of states (DOS) diagram in metal–adsorbate adsorption [9, 49, 62]

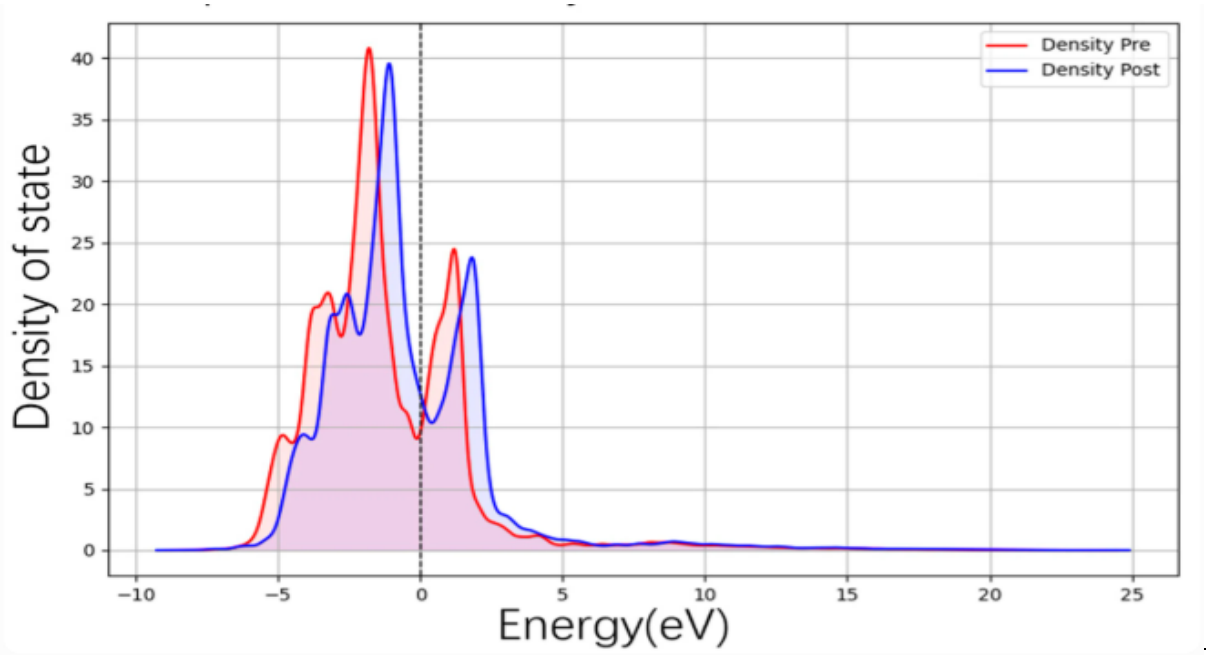

Figure 5. Comparative diagram of the density of states (DOS) before and after a perturbation